INTERNAL CONSISTENCY FOR XCT-DERIVED ESTIMATES OF FORMATION ORIENTATION OF LUNAR BASALTS 12038 AND 15556. J.H.C. De Oliveira[1] and C.R. Neal[2], [1,2]University of Notre Dame, Notre Dame IN, 46556 ([1]jdeolive@nd.edu; [2]cneal@nd.edu).

Introduction: Micro X-Ray Computed Tomography (XCT) is a nondestructive method of imaging that has been applied to rocks to observe internal features. An XCT scan of a rock produces a series of slices (images in grayscale). Different features are delineated by shades of gray ranging from black to white [1]. The XCT data used here were for low-Ti basalts 12038,7 and 15556,0 and were downloaded from NASA's Astromaterials 3D website [2].

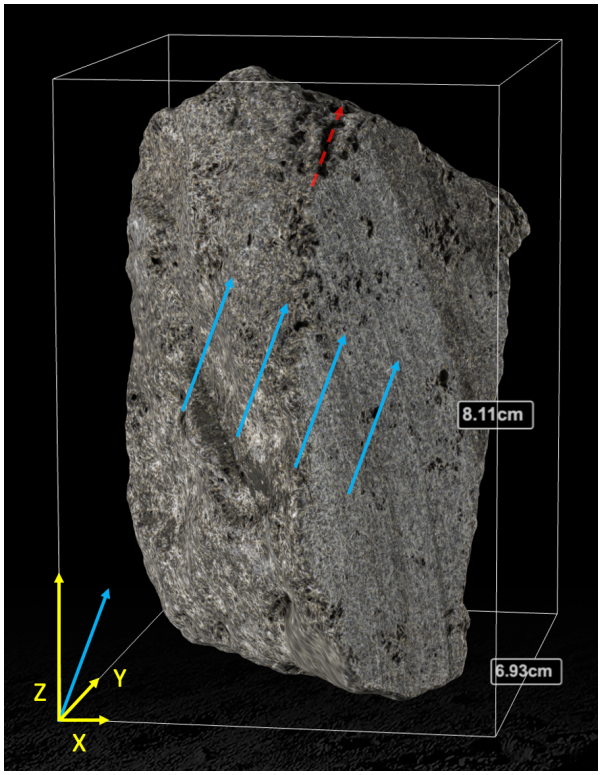

Figure 1. Three-dimensional vector (blue arrows) indicative of the vertical orientation at formation overlaid on lunar basalt 12038,7. Potential pipe vesicle overlaid by dotted red arrow.

The XCT scans provide researchers with the ability to observe and quantify fracture geometry and void space distributions throughout sample. Trends in void space (vesicle) proportions throughout a lava flow can be indicative of sample orientation at formation (see Figs. 1 and 2), and relative abundance gives an indication of the minimum volatile content of the magma [3]. It is for this reason that it is a topic of great interest in volcanology [4].

This study seeks to build off our preliminary study [5] by refining the software and in particular, the accuracy and internal consistency of the measurements.

Methodology: XCT images were downloaded from the Astromaterials 3D website [2], with additional axes data provided directly by Erika Blumenfeld.

The software developed for this project uses *Python* and the library *OpenCV* to bulk process the images and derive the data explored here.

A similar protocol was used in our previous study [5], in which the image background was removed by masking using a binary threshold. After background removal, grayscale histograms were produced. These

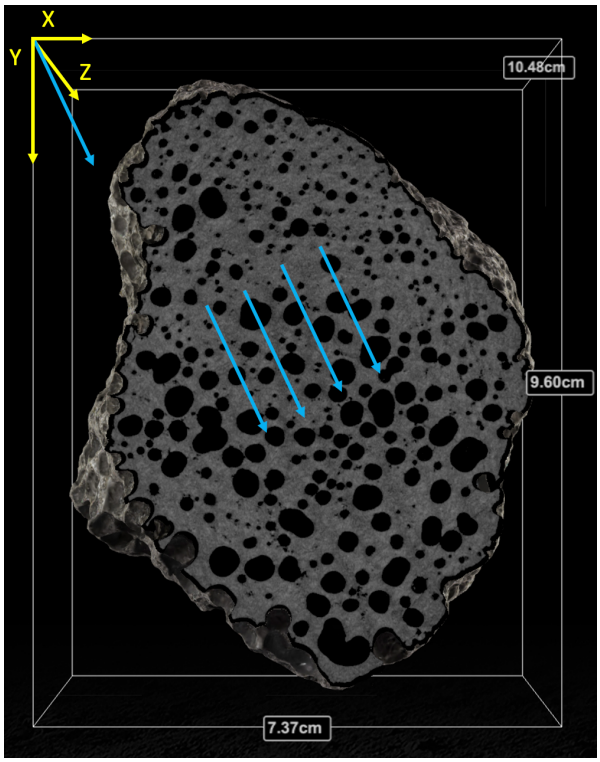

Figure 2. 15556,0 XCT slice (z axis going into the page) with blue vectors indicating hypothesized vertical orientation at formation. Notice the change in vesicle abundance and size.

are plots of pixel color (from 0 to 255 — i.e., from black to white) by number of pixels. Determining void space proportion for a single XCT slice was then simple: divide the amount of void space by the amount of rock (i.e., divide the number of pixels with a value of 0 by the sum of all pixels whose values range from 1-254).

This process was automatically repeated by the software for each XCT slice (over a thousand images for each axis), and the resulting proportions plotted.

A second-degree polynomial fit was assigned to each proportion plot — the resulting r^2 was subtracted from 1 and this value was used as the vector magnitude

for the corresponding axis. This differs from last year's study [5] in which the data was fitted linearly, and the r^2 value was used as a proxy for vector magnitude.

Discussion: Threshold values affect the fidelity of the proportion plots. A lower threshold value can result in background pixels (non-rock information) being preserved, whereas a higher threshold value can result in rock being removed. Either way, threshold masking induces some error, and there remains no perfect way to select an ideal threshold value.

A method that produces similar results for a range of reasonable threshold values is the goal as it demonstrates that the induced error from threshold masking is minimized. With the analyses used in [5], this was not the case. The hypothesized vertical orientation at formation varied greatly depending on the threshold value selected for image processing.

The new analysis method produces far more consistent results (Fig. 3). Its superiority is rooted in two changes: 1) switching from void space divided by rock space per slice to void space per slice divided by total rock space 2) using parabolic trendlines instead of linear. These two changes produced data that were far more consistent than our original results [5].

This alone is not good justification for the method's accuracy or use, however. Physical features were used in conjunction with these results to demonstrate a causal relationship with our estimated void space gradient (i.e., the data produced describes the physical reality of the samples). The first qualitative measure was that of the void space itself; the vectors produced from this software are consistent with the gradational changes in void space throughout these two samples. The second measure was only applied to 12038,7, where void space defines pipe vesicles (e.g., [6]). The clearest "pipe" appears near the top of the rock and follows a similar trajectory to the 3D vector produced by the software. Such features suggest that the vectors are sound.

Conclusion: Increased internal consistency within the data produced suggests a higher fidelity in our analyses. Ultimately, the best test of this method would be on terrestrial basalts with a known vertical orientation at formation and will remain a possible pathway for future research. Another test could involve reslicing the XCT data along new axes to determine if the results are the same. Textural information within the samples themselves can also provide further evidence in favor of the produced measurements. Future work will focus primarily on releasing the software under an open-source license for use by the scientific community and quantifying minimum volatile contents for samples.

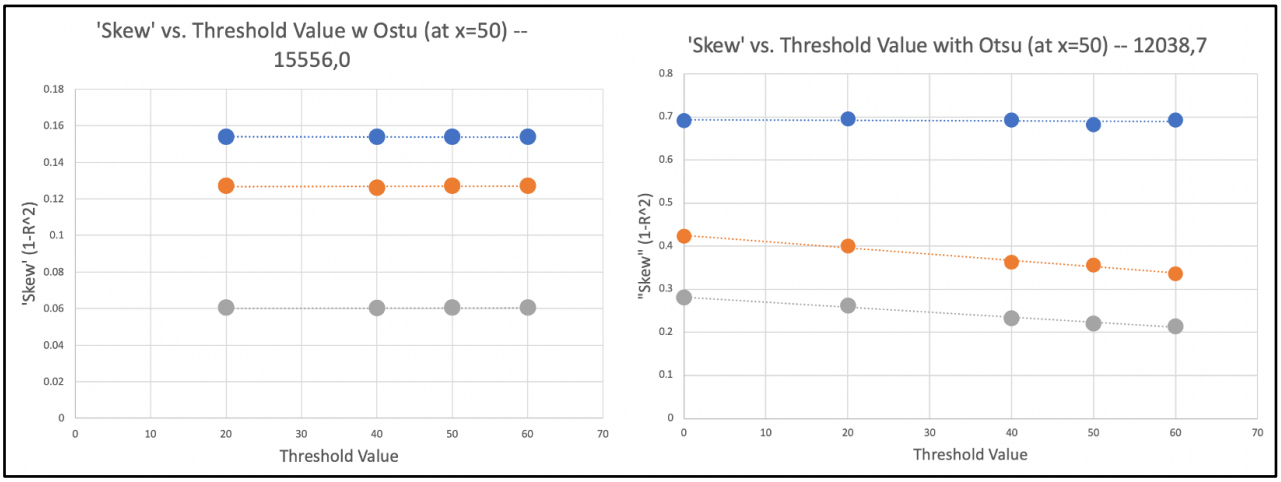

Figure 3. Plots of 'Skew' vs. Threshold Value for 15556,0 and 12038,7 (x-axis:gray, y-axis:orange, z-axis:blue). 15556,0 has more relative consistency between the axes, while 12038,7 has consistency only between the y and x axes. This is likely because the z-axis had a far greater amount of void space compared to the other two axes. Skew produced using a threshold determined by Otsu binarization is displayed on the x = 50 point on both plots. Otsu binarization is a method for determining an "ideal" threshold [7].

Acknowledgments: These XCT image data were produced by Astromaterials 3D for NASA's Acquisition & Curation Office and were funded by NASA Planetary Data Archiving, Restoration, and Tools Program, Proposal No.: 15-PDART15_2-0041. Scanned for Astromaterials 3D at the University of Texas High-Resolution X-Ray CT Facility by Matthew Colbert on 28 June 2016.

References: [1] Deng H. et al. (2016) *Computational Geosciences* 20, 231-244. [2] Astromaterials 3D. https://ares.jsc.nasa.gov/astromaterials3d/apollo-lunar.htm [3] Shea T. et al. (2010) *Journal of Volcanology and Geothermal Research* 190, 271-289. [4] Wilbur Z.E. et al. (2020) LPSC 51 #2236. [5] De Oliveira et al. (2021) LPSC52, #2628; [6] Self S. et al. (1998) *Annu. Rev. Earth Planet Sci.* 26, 81-110. [7] N. Otsu (1979 *IEEE Transactions on Systems, Man, and Cybernetics* 9, 62-66.